THE JOURNAL OF PHYSICAL CHEMISTRY A

Article

pubs.acs.org/JPCA

Synthesis and Optical Properties of Pyrrolo[3,2-*b*]pyrrole-2,5(1*H*,4*H*)-dione (iDPP)-Based Molecules

Mindaugas Kirkus,[†] Stefan Knippenberg,[‡] David Beljonne,[‡] Jérôme Cornil,[‡] René A. J. Janssen,[†] and Stefan C. J. Meskers*[,†]

[†]Molecular Materials and Nanosystems, Eindhoven University of Technology, P.O. Box 513, 5600 MB Eindhoven, The Netherlands

[‡]Laboratory for Chemistry of Novel Materials, University of Mons, Place du Parc 20, B-7000 Mons, Belgium

Supporting Information

ABSTRACT: We describe the synthesis and photophysical properties of a series of derivatives of pyrrolo[3,2-*b*]pyrrole-2,5(1*H*,4*H*)-dione-3,6-diyl (iDPP) linked to two oligothiophenes of variable length (*n*T). The iso-DPP-oligothiophenes (iDPP*n*Ts) differ from the common pyrrolo[3,4-*c*]pyrrole-1,4(2*H*,5*H*)-dione-3,6-diyl-oligothiophene analogues (DPP*n*Ts) by a different orientation of the two lactam rings in the bicyclic iDPP unit compared to DPP. In contrast to the highly fluorescent DPP*n*Ts, the new isomeric iDPP*n*Ts exhibit only very weak fluorescence. We demonstrate with the help of quantum-chemical calculations that this can be attributed to a different symmetry of the lowest excited state in iDPP*n*T (*A* in C_2 symmetry) compared to DPP*n*Ts (*B*) and the corresponding loss in oscillator strength of the lowest energy transition. Upon extending the oligothiophene moiety in the iDPP*n*Ts molecules, the charge transfer character of the lowest *A* excited state becomes more pronounced. This tends to preclude high fluorescence quantum yields even in extended iDPP*n*Ts systems.

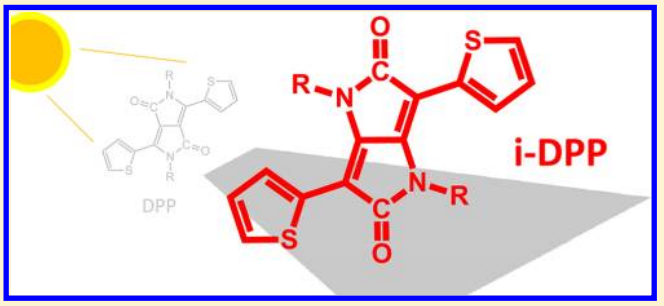

INTRODUCTION

The pyrrolo[3,4-*c*]pyrrole-1,4-dione-3,6-diyl (DPP, Figure 1) chromophore, first reported in 1974,[1] has recently emerged as an important and versatile building block for organic π-conjugated polymers and extended π-systems with interesting opto-electronic properties that find application in organic solar cells and thin-film transistors.[2] DPP-based molecules have several desirable optical properties such as high extinction coefficients, readily tunable absorption wavelength, and bright fluorescence.[3,4] The usefulness and versatility of the DPP unit has inspired the search for related chromophores. In this research, we focus on the isomeric pyrrolo[3,2-*b*]pyrrole-2,5-dione-3,6-diyl (iDPP) which is a natural derivative of the pulvinic acid (Figure 1)[5,6] and used as a pigment.[7]

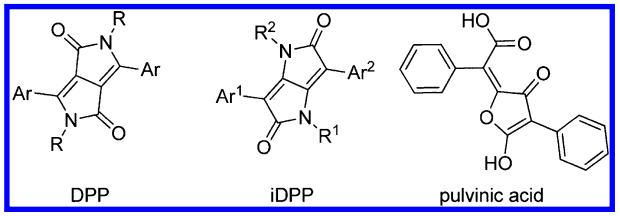

Figure 1. Chemical structures of 3,6-diaryl-pyrrolo[3,4-*c*]pyrrole-1,4-dione (DPP), 3,6-diaryl-pyrrolo[3,2-*b*]pyrrole-2,5-dione (iDPP), and pulvinic acid.

The first synthesis of the symmetrical and asymmetrical pyrrolo[3,2-*b*]pyrrole-2,5-diones (iDPPs, $Ar^1 = Ar^2$ = aryl and $R^1 = R^2$ = H, Figure 1) has been reported by Fürstenwerth,[8] starting from pulvinic acid derivatives using harsh reaction conditions in low reaction yields due to formation of side products. A number of symmetrical *N*-arylated iDPPs ($R^1 = R^2$ = Ar and $Ar^1 = Ar^2$, Figure 1) have been synthesized by reacting aromatic ester carbanions with aromatic oxalic acid−bis-(imidoyl)dichlorides[9] that can be obtained in a one-pot reaction from aromatic amines, oxalyl chloride, and PCl_5.[10,11] Asymmetrical *N*-arylated iDPPs (R^1, R^2 = aryl with $R^1 \neq R^2$ and $Ar^1 = Ar^2$) have been prepared by the same synthetic strategy[12] but using asymmetrical oxalic acid−bis(imidoyl)dichlorides which can be prepared in a few steps starting from commercial ethyl-2-chloro-2-oxoacetate and different derivatives of aniline.[13]

The nature of the lowest excited state in DPP and iDPP derivatives is of importance for application in opto-electronics. While normal DPPs are renowned for their bright fluorescence in solution,[14,15] many structurally related chromophores show hardly any photoluminescence activity. For example, recent studies on benzodipyrrolidones revealed that these molecules show essentially no fluorescence.[16] Similarly low fluorescence quantum yields (from 0.3% to 2%) were reported for

Received: January 9, 2013
Revised: March 4, 2013

   dx.doi.org/10.1021/jp400256s | *J. Phys. Chem. A* XXXX, XXX, XXX−XXX

Scheme 1. Synthesis of Pyrrolo[3,2-*b*]pyrrole-2,5-dione-Based *N*-Arylated Derivatives T1, T2, and T3[a]

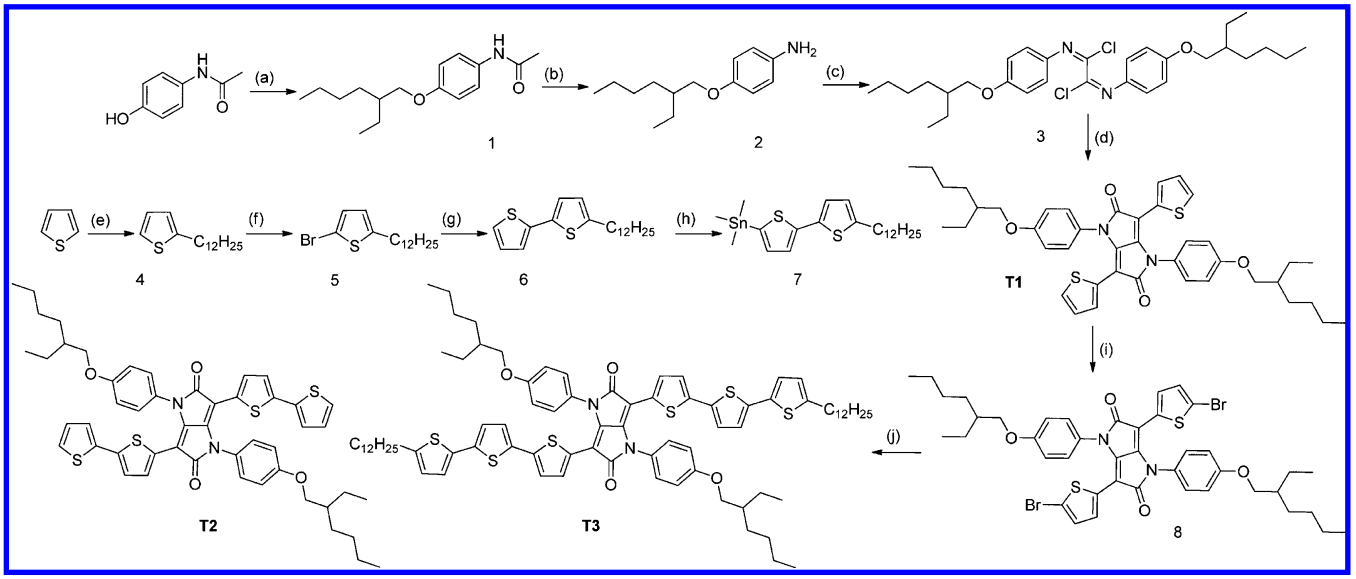

[a](a) K_2CO_3, 2-ethylhexyl bromide, 2-butanone, reflux, 12 h; (b) ethanol, HCl, reflux, 12 h; (c) oxalyl chloride, toluene, rt, 30 min; PCl_5, reflux, 1 h; (d) diisopropylamine, 2.5 M BuLi in *n*-hexane, THF, −78 °C; then ethyl-2-thiopheneacetate, rt, 12 h; (e) 2.5 M BuLi in *n*-hexane, THF, −78 °C, 1.5 h, −78 °C, rt, $C_{12}H_{25}Br$, reflux, 2 days; (f) NBS, AcOH/chloroform, 0 °C; then rt, 12 h; (g) Mg, 2-bromothiophene, Et_2O, rt; then 50 °C, 4 h; (**6**), $Pd(dppf)Cl_2$, Et_2O, 0−5 °C, rt, overnight; (h) 2.5 M BuLi in *n*-hexane, THF, −78 °C, 30 min; then rt, 30 min; then −78 °C, trimethyltin chloride, rt, overnight; (i) NBS, 50 °C, 12 h; (j) 2-(tributylstannyl)thiophene or **8**, $Pd[PPh_3]_4$, toluene, 100 °C, 36 h.

benzodifuranone derivatives[17] as well as for iDPP polymers (<1%) .[18] For 3,6-diphenyl-2,5-dihydropyrrolo[3,2-*b*]pyrrole-2,5-dione (iDPP, $R^1 = R^2 = H$, $Ar^1 = Ar^2 = Ph$) fluorescence could not be observed, which was related to the forbidden nature of the lowest electronic transition.[19]

Quantum-chemical calculations based on density functional theory (DFT) performed on the isomeric linear benzodifuranones, benzodipyrrolinones, and their homologues[20] indicate the presence of low-energy n−π^* states in these π-conjugated systems. From the experimental studies on azoaromatics,[21,22] e.g., acridine, it is well known that if the lowest excited state is of n−π^* nature, the fluorescence quantum yield is negatively affected. In this case, the low quantum yield is attributed to efficient intersystem crossing to the triplet states. Even if the lowest excited state in a π-conjugated molecule is of the desired orbital nature (π−π^*), the fluorescence yield can still be very low. This is the case for, e.g., polyenes,[23−25] polydiacetylenes,[26,27] polythienylenevinylenes,[28] and retinal.[29,30] In contrast, π-conjugated polymers and oligomers of phenylenevinylene, phenyleneethynylene, thiophene, and fluorene show very bright fluorescence. This is generally attributed to the symmetry of the lowest excited state. Assuming the C_2 point group for the π-systems, the lowest π−π^* excited singlet state in the nonfluorescent molecules is assigned to the *A* symmetry while for the fluorescent materials the lowest excited singlet state has *B* character. The energy difference between *A* and *B* excited singlet states can be small; in such cases, small alterations in chemical structure or the environment of the molecule can have a drastic influence on the fluorescence properties.

Here, we describe the synthesis of three 3,6-bis(oligothiophene)pyrrolo[3,2-*b*]pyrrole-2,5-dione (iDPP*n*T, *n* = 1−3) derivatives and investigate their optical properties in detail using experimental and theoretical methods. We find that these molecules fluoresce but with very low quantum yield (10^{-3}−10^{-4}). We attribute the low fluorescence to emission from the lowest, A-symmetry, singlet excited state in these oligothiophene-substituted iDPP*n*Ts. The energy gap between *A* and *B* excited states decreases with the number of thiophene rings in the oligothiophene substituent. We observe, however, only a very moderate improvement in the transition dipole strength for the $S_1 \rightarrow S_0$ transition in the extended systems. Development of substantial intramolecular charge transfer character in the lowest excited state of the larger systems appears to preclude a strong increase in the fluorescence quantum yield.

RESULTS AND DISCUSSION

Synthesis. The structure and synthesis of iDPP*n*Ts **T1**−**T3** with a different number of thiophene rings in the backbone are shown in Scheme 1. For preparation of **T1**−**T3** we used a synthetic strategy reported by Langer et al.[11,13] To increase the solubility of the compounds we included 2-ethylhexyloxy substituents on the *N*-phenyls. The corresponding aniline derivative **2** was synthesized from commercial 4-acetoamidophenol using Williamson ether synthesis,[31] followed by deacylation of the amide using concentrated hydrochloric acid in ethanol resulting in **2**. Synthesis of the symmetric oxalic acid−bis(imidoyl)dichloride was performed in a one-pot reaction of oxalyl chloride with **2**, followed by treatment with anhydrous PCl_5 in boiling toluene. Although many oxalic acid bis-alkyl derivatives can be purified by recrystallization from propylencarbonate, the resulting oily intermediate **3** did not crystallize and was used in the next step without purification.

Reaction of **3** with the enolate of ethyl-2-thiopheneacetate prepared by treatment with lithium diisopropylamide (LDA) resulted in the iDPP derivative **T1** in high (68%) yield. Derivatives **T2** and **T3** could be obtained by further functionalization of **T1**. To this end, **T1** was first brominated with NBS in chloroform at 50 °C and the resulting dibromo compound **8** was used in Stille couplings with the organotin derivatives of either a thiophene or a 2,2′-bithiophene **7**.

dx.doi.org/10.1021/jp400256s | J. Phys. Chem. A XXXX, XXX, XXX−XXX

Derivative **7** was prepared by alkylation of the thiophene using *n*-BuLi and the corresponding alkyl halide, followed by bromination and Kumada coupling, resulting in monoalkylated 2,2′-bithiophene derivative **6**. Usually bis(diphenylphosphino)-propane nickel(II) chloride (Ni[dppp]Cl_2) is used in Kumada couplings as a catalyst.[32,33] In our synthesis we used [1,1′-bis(diphenylphosphino)ferrocene]dichloropalladium (Pd-[dppf]Cl_2) as a catalyst because it is more active compared to Ni[dppp]Cl_2, giving higher yields, shorter reaction times, and higher purity of the target derivative **6**.[34] Stannylation reaction of **6** with trimethyltin chloride in anhydrous THF gave analytically pure trimethylstannane derivative **7** in high (89%) yield. Finally, Stille coupling[35] was used for synthesis of the target compounds **T2** and **T3** using Pd[PPh_3]$_4$ as a catalyst. **T2** and **T3** could be obtained in low yields. The Stille reaction is often an efficient method for C−C coupling between DPPs and the electron-rich units. Stille coupling has, for instance, been used to synthesize small DPP molecules[36−39] and high molecular weight DPP polymers.[40−44] In contrast, the final C−C coupling reactions to get **T1** and **T2** proceeded with only low yields, illustrating the need for further optimization. Curiously, there are very few examples in the literature of C−C coupling reactions between dibromo derivatives of pyrrolo[3,2-*b*]pyrrole-2,5-diones and stannyl derivatives or bispinacolboronic esters of electron-rich aromatic units. For synthesis of the π-conjugated polymers containing pyrrolo[3,2-*b*]pyrrole-2,5-diones, Suzuki coupling was used as described by Welerlich et al.[18] However, the indices of polydispersity (PDI) are around 5.6, thus showing that the Suzuki reaction conditions are not ideal for this chromophore. The iDPP polymers reported in a recent patent were prepared by Stille couplings using $Pd_2(dba)_3$/(*o*-tol)$_3$P as a catalytic system.[45] The structure and purity of the intermediate and final compounds were determined by MALDI-TOF, ^{13}C NMR, and ^{1}H NMR techniques.

Quantum-Chemical Calculations. Quantum-chemical calculations were performed on an analogue of **T1** to find the low-energy conformations of the electronic ground state of the iDPP moiety. To simplify the calculations, the two alkoxy substituents on the phenyl moieties were replaced with hydrogen atoms. The ground state geometry of the **T1** analogue was optimized at the second-order Møller−Plesset (MP2) level along with the Pople 6-31G* basis set with 520 basis functions using the Gaussian09 quantum-chemistry program.[46] Two conformers have been identified (Figure 2). The first conformer (Figure 2a) has C_2 symmetry, while the other conformer has C_i symmetry (Figure 2b). The C_i isomer is only 0.6 kcal/mol higher in energy than the C_2 isomer. A similar result was recently found for a iDPP-type molecule where the thiophenes are replaced by hydrogen.[19]

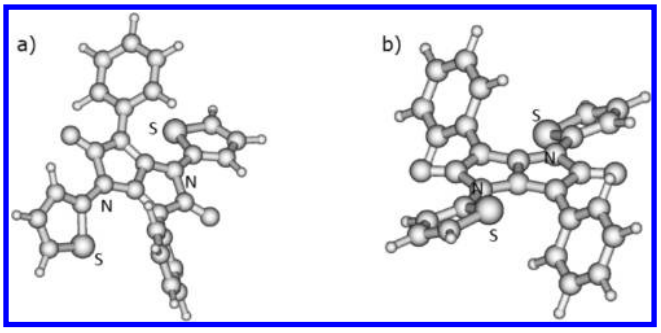

Figure 2. Two low-energy ground-state conformers of the T1 derivative, as identified at the MP2/6-31G* level of theory: (a) C_2 and (b) C_i symmetry structures.

To investigate the nature of the lowest two excited states, approximate second-order coupled cluster (CC2),[47−49] equation of motion-coupled cluster singles and doubles (EOM-CCSD),[50] and time-dependent density functional theory calculations (TD-DFT) along with the long-range-corrected ωB97xd[51] and ωPBE[52] functionals have been performed using Turbomole 5.10,[53] Molpro 2009,[54] and Q-Chem 4.0,[55] consistently relying on the 6-31G* basis set. The reliability of the excitation energies obtained at the TD-DFT level is substantiated by the so-called Λ overlap parameter proposed by Peach et al.,[56] which measures the degree of CT character and hence the probability of a CT-related failure of TDDFT. For the lowest two single excited states of both conformers of iDPP, Λ is comfortably large and supports therefore the analysis given here.

For the C_2 and C_i conformers, the lowest singlet excited state, S_1, is very similar in energy and orbital nature (Table 1). The same holds for the second singlet excited state, S_2. TD-DFT as well as ab initio methods yield $\pi-\pi^*$ character for S_1 and S_2 of both conformers. For the C_2 conformer, the Hartree−Fock orbitals are illustrated in Figure 3. Focusing on the central butadiene part of the pyrrolopyrrole fused ring system, the HOMO−1 corresponds to the lowest occupied π-orbital for a butadiene segment. The HOMO has the expected bonding interaction over the double bonds, whereas the LUMO has nodes over the double bonds and a bonding character over the central C−C bond (Figure 3). The S_1 state is built on the HOMO−1→ LUMO excitation, while S_2 has HOMO → LUMO character. The S_1 (A_g) ← S_0 (A_g) transition in the C_i conformer is dipole forbidden because both the initial and the final states have A_g character; S_2 (A_u) ← S_0 (A_g) is dipole allowed and predicted to have an oscillator strength close to unity (Table 1). For the C_2 conformer, both transitions are formally dipole allowed, though an extremely low oscillator strength is predicted for $S_1(A)$ ← $S_0(A)$ (Table 1). The transition dipole moment for this transition is perpendicular to the plane of the central fused ring unit and therefore small in magnitude. For the $S_2(B)$ ← $S_0(A)$ transition, a large oscillator strength is predicted.

Optical Properties. Room-temperature (298 K) absorption, fluorescence, and fluorescence excitation spectra of **T1**, **T2,** and **T3** in solvents of increasing polarity (toluene (Tol), *o*-dichlorobenzene (*o*-DCB), and benzonitrile (BZN)) are shown in Figure 4. Corresponding data can be found in Table 2.

The absorption spectrum of **T1** in toluene features an intense broad absorption band in the visible range with a maximum around 2.95 eV and molar decadic absorption coefficient ε_{max} of 22 × 10^3 M^{-1} cm^{-1}. The magnitude of ε_{max} points to an optically allowed $\pi-\pi^*$ transition. Therefore, we assign the 2.95 eV absorption band to a transition from the 1^1A ground state to an excited singlet state of *B* symmetry ($^1B^*$), adopting the C_2 point group for the chromophore. Notably, below 2.6 eV, the absorption spectrum of **T1** shows a low-intensity shoulder at the low-energy side of the allowed $^1B^*$ ← 1^1A transition. The absorption coefficient for this low-energy shoulder of **T1** at 2.43 eV is only 1.8 × 10^3 M^{-1} cm^{-1}.

A possible explanation for the weak intensity shoulder below 2.6 eV in the absorption spectrum of **T1** could be a conformational equilibrium of the molecule in the room-temperature solution. For instance, thiophene-substituted DPP

dx.doi.org/10.1021/jp400256s | J. Phys. Chem. A XXXX, XXX, XXX−XXX

Table 1. Vertical Excitation Energies from the Ground State to the Lowest Two Excited States of the Two Conformers of T1 Shown in Figure 2 (with C_2 and C_i symmetry), As Computed at Different Levels of Theory[a]

	C_2							
method	$E[S_1(A)]$ (eV)[b]	f	$E[S_2(B)]$ (eV)[c]	f	$E[S_3(A)]$ (eV)	f	$E[S_4(B)]$ (eV)	f
ωB97xd	2.70[d]	0.004	3.18[e]	0.607	3.87 ($n\pi^*$)	0.002	4.20	0.102
ωPBE	2.76	0.004	3.22	0.623	3.92 ($n\pi^*$)	0.002	4.27	0.104
CC2	2.75		3.36		3.75 ($n\pi^*$)			
EOM-CCSD	3.13		3.72					
	C_i							
method	$E[S_1(A_g)]$ (eV)[b]	f	$E[S_2(A_u)]$ (eV)[c]	f	$E[S_3(A_u)]$ (eV)	f	$E[S_4(A_u)]$ (eV)	f
ωB97xd	2.68[f]	0	3.18[g]	0.586	3.90 ($n\pi^*$)	0.046	4.34	0.106
ωPBE	2.73	0	3.23	0.604	3.95 ($n\pi^*$)	0.046	4.41	0.110
CC2	2.73		3.37		3.78 ($n\pi^*$)			
EOM-CCSD	3.11		3.74					

[a] f is the oscillator strength. [b] H−1 → L (π−π^*) excitation. [c] H → L (π−π^*) excitation. [d] $\Lambda = 0.698$. [e] $\Lambda = 0.850$. [f] $\Lambda = 0.561$. [g] $\Lambda = 0.654$. Excited states are of $\pi\pi^*$ nature, except where indicated.

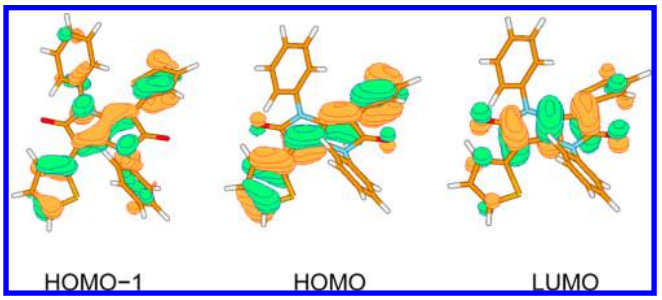

Figure 3. Hartree−Fock orbitals involved in the S_1 and S_2 excitations of the **T1** analogue with C_2 symmetry.

(DPP1T) shows a narrowing of the widths of the peaks upon cooling (Figure 5, bottom) due to planarization of the molecules with the appearance of the distinct vibronic peaks separated by ~0.18 eV, which can be attributed to the change in the C−C bond length alternation of the π-conjugated system after excitation.[58,59] The red shift in the absorption of DPP1T upon cooling can be explained by the more planar structure of the molecules, leading to increased π-conjugation, which is known for various thiophene derivatives.[59]

The absorption spectrum for **T1** was investigated at variable temperatures, and results are shown in Figure 5 (top). As can be seen, upon lowering the temperature the main $^1B^* \leftarrow 1^1A$ UV band near 2.95 eV sharpens somewhat and shows some vibronic fine structure at 80 K. The low-energy shoulder below 2.6 eV persists at low temperature. We thus conclude that the low-energy absorption tail in the room-temperature absorption spectrum of **T1** is not the result of a conformational equilibrium in the molecule. For **T2** and **T3** similar changes occur when reducing the temperature. The absorption bands remain broad and do not show clear vibronic structure.

In toluene, **T1** shows a weak fluorescence featuring a broad fluorescence band centered around 1.8 eV (Figure 4). The fluorescence quantum yield ϕ_{flu} is very low. The low yield implies efficient nonradiative decay pathways of the excited state, which are common for carbonyl-containing chromophores.[60−64] Using Rhodamine 101 as a standard,[65] we determine ϕ_{flu} to be on the order of 10^{-4} (Table 2). In more polar solvents like *o*-DCB and BZN the fluorescence quantum

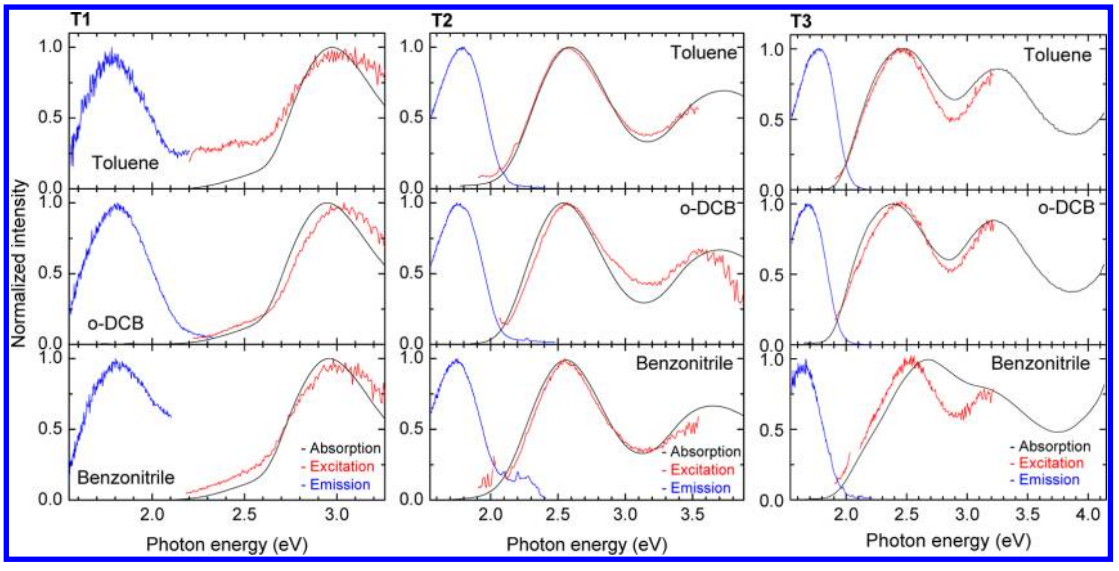

Figure 4. Room-temperature absorption (black line), excitation (red line), and emission (blue line) spectra of **T1**, **T2**, and **T3** in dilute (OD < 0.1) toluene, *o*-DCB, and benzonitrile solutions. Excitation photon energies: T1 2.8 (toluene, *o*-DCB) and 3.02 eV (benzonitrile); T2 2.5 eV; T3 2.3 eV.

dx.doi.org/10.1021/jp400256s | J. Phys. Chem. A XXXX, XXX, XXX−XXX

Table 2. UV−Vis Absorption and Fluorescence Data in Organic Solvents of Different Polarity for T1, T2, and T3 at 298 K

		abs		flu						
compound	solvent	E_{ons} [a] (eV)	E_{max} [b] (eV)	E_{max} [b] (eV)	ε_{max} [c] ($M^{-1}cm^{-1}$)	τ_{PL} [d] (ns)	ϕ_{flu} [e]	k_{rad} (μs^{-1})	k_{nrad} (ns^{-1})	$^1B^* \rightarrow {}^1A$ k_{rad} [f] (μs^{-1})
T1	Tol	2.18	2.97	1.80		0.64	7×10^{-4}	1.1	1.6	
	o-DCB	2.17	2.94	1.81	21 845	0.45	4×10^{-4}	0.9	2.2	1.1×10^2
	BZN	2.17	2.95	1.80		0.27	2×10^{-4}	0.7	3.7	
T2	Tol	2.09	2.59	1.79		1.0	8×10^{-3}	8	1.0	
	o-DCB	2.07	2.54	1.74	22 232	0.77	5×10^{-3}	6	1.3	1.3×10^2
	BZN	2.10	2.56	1.75		0.64	3×10^{-3}	5	1.6	
T3	Tol	2.00	2.48	1.78		1.0	2×10^{-2}	20	1.0	
	o-DCB	1.92	2.38	1.70		0.80	9×10^{-3}	11	1.3	
	BZN	1.92	2.67	1.66		0.60	3×10^{-3}	5	1.7	

[a]Onset of absorption spectra measured at 298 K. [b]Absorption and emission maxima measured at 298 K. [c]Extinction coefficient calculated from the maximum of the absorption at 298 K. [d]Lifetime of the emission approximated with a single-exponential function at 298 K. [e]Relative to Rhodamine 101, excitation photon energy = 2.79 eV. [f]Calculated using the Strickler−Berg equation.[57]

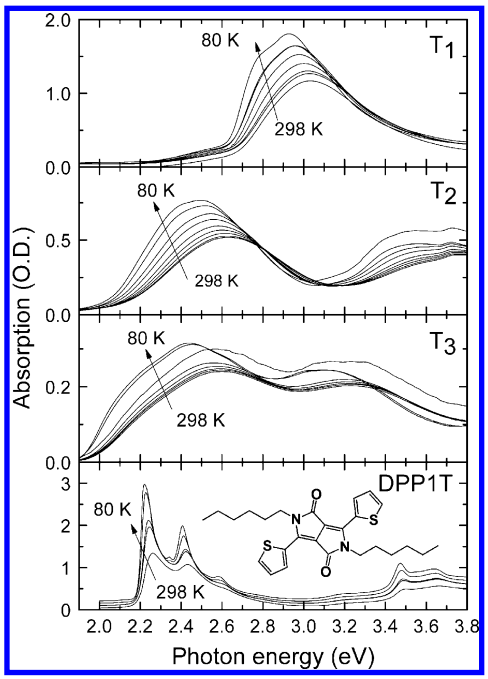

Figure 5. Variable-temperature UV−vis absorption of **T1**, **T2**, **T3**, and **DPP1T** in dilute 2-methyltetrahydrofuran solutions.

yield is even lower. To ensure that the weak fluorescence signals observed are indeed due to the **T1**, **T2**, and **T3** molecules, fluorescence excitation spectra were measured at low optical densities for all compounds and compared to the absorption spectra in the same solvent (Figure 4). We find that absorption and excitation traces overlap nicely, which firmly supports the assignment of the weak fluorescence signals to the iDPP*n*T molecules.

The weak fluorescence band of **T1** overlaps with the weak low-energy shoulder in the absorption spectrum and appears to be unrelated to the allowed $^1B^* \leftarrow 1^1A$ transition at 2.95 eV. This suggests that the fluorescence and low-energy absorption shoulder arise from an electronic transition different from the $^1B \leftarrow 1^1A$ transition band, as suggested by the theoretical calculations. Fluorescence of **T1** decays approximately exponentially in time after pulsed excitation at 4.0 eV with an excited state lifetime of 0.64 ns (Table 2). From the measured fluorescence lifetime and the fluorescence quantum yield we calculate the rate of radiative decay (k_{rad}) in *o*-DCB and find a value of 0.9 μs (Table 2). This small value of k_{rad} is consistent with an optically forbidden but spin-allowed $S_1 \rightarrow S_0$ transition.

The experimentally determined radiative rate may be compared to the radiative rate predicted from the absorption spectrum in *o*-DCB using the Strickler−Berg relation,[57] assuming that all the oscillator strength in the visible absorption band below 3.2 eV is also available for the emissive transition. For **T1** we integrate the absorption spectrum over the 3.2−2.2 eV energy range and predict a radiative rate constant 0.1 ns^{-1}. This is more than 2 orders of magnitude higher than the experimental value (9×10^{-4} ns^{-1}) and clearly shows that the main absorption band with maximum at 2.95 eV generates an excited state that is different from the excited state, giving rise to the fluorescence.

On the basis of the small rate for radiative decay, we assign the fluorescence to a $2^1A^* \rightarrow 1^1A$ transition. The low-energy, low-intensity shoulder in the absorption at 2.5 eV is then assigned to the reverse transition ($2^1A^* \leftarrow 1^1A$) and the main absorption band at 2.95 eV to $1^1B^* \leftarrow 1^1A$. In this assignment, the S_1 excited state is assumed to be of $\pi-\pi^*$ orbital nature, as supported by theory. Alternatively, a lowest excited singlet state of n$-\pi^*$ character could also explain the small radiative decay rate for the lowest excited state. However, ^{1}n$-\pi^*$ excited states with energy below 2.0 eV are uncommon in organic molecules. For linear polyenal molecules, ^{1}n$-\pi^*$ states occur with energy about 3.0 eV above the ground state.[66,67] For retinal, the ^{1}n$-\pi^*$ and ^1A_g*state are close in energy and both these states are below the ^1B_u* state.[29,68−70] The weak fluorescence from 2,4,6,8,10-dodecapentaenal has been assigned to $2^1A_g^* \rightarrow 1^1A_g$.[71] For longer polyenals, it has been argued that the singlet $\pi-\pi^*$ excited state of ^1A_g* symmetry is lower in energy than the ^{1}n$-\pi^*$ state. It should be noted that upon lowering the symmetry from C_{2h} to, e.g., C_2, extensive mixing of n$-\pi^*$ and $\pi-\pi^*$ states could occur and it may no longer be meaningful to distinguish n$-\pi^*$ and $\pi-\pi^*$ states. At the B97xd/6-31G* level of theory for both the C_2 and C_i conformers, the first state with a solid n$-\pi^*$ character is the S_3 state (S_4 is $\pi-\pi^*$). Furthermore, especially in polar solvents, the picture may be further complicated by the presence of low-lying charge transfer (CT) like excited states which have been found in carotenoids.[72,73] The decrease in radiative and increase in nonradiative decay rate for **T1** upon increasing the polarity of the solvents (see Table 2) provides an indication for involvement of the CT state in the photophysical behavior. The photon energy corresponding to the maximum of the fluorescence intensity, however, does not shift appreciably with

dx.doi.org/10.1021/jp400256s | J. Phys. Chem. A XXXX, XXX, XXX−XXX

increasing solvent polarity. The absence of such a shift suggests a limited CT character in the lowest excited state; still the CT state could be involved in the decay from S_1 to S_0 as a transition state.

Upon extending the conjugation length in these molecules by adding more electron-rich thiophene rings (compounds **T2** and **T3**), the main absorption maximum in the visible range shifts to lower energy and is located at 2.6 and 2.5 eV, respectively (Figure 4). For **T2** and **T3,** we also assign the main absorption band in the visible range to the $1^1B^* \leftarrow 1^1A$ transition. For **T2** the low-energy absorption shoulder below the $1^1B^* \leftarrow 1^1A$ band is more pronounced compared to **T1**. For **T3**, the shoulder is almost invisible. The fluorescence quantum yield for **T2** and **T3** remains low (<0.1) but increases approximately by 1 order of magnitude for each pair of additional thiophene rings in the oligothiophene substituents (Table 2). The fluorescence lifetimes for **T2** and **T3** are in the nanosecond time domain. Rates for radiative decay remain small considering the size of the conjugated system and indicate a forbidden nature for the fluorescent transition. Therefore, we assign the lowest excited state S_1 in all three oligomers to the 2^1A^* state. The increase in radiative decay rate with increasing number of thiophene rings may then be ascribed to more efficient vibronic mixing of the 1^1B^* and 2^1A^* states facilitated by their smaller energy difference. The assignments of the lowest excited states of **T1**, **T2**, and **T3** are summarized in Figure 6. Comparing the

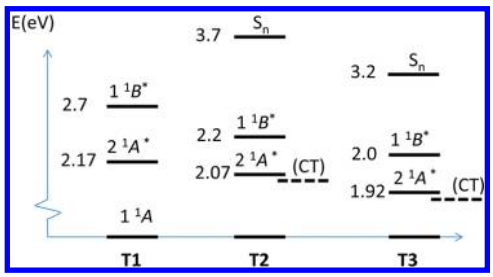

Figure 6. Jablonski diagram showing the estimated energetic positions of the singlet excited states of **T1**, **T2**, and **T3**. For **T2** and **T3** the CT character of the relaxed lowest excited state in polar solvent is indicated by the dashed line. Numbers in italics correspond to energies tentatively assigned to excited singlet states associated with the oligothiophene moiety.

energies of $^1B^*$ and $^1A^*$ excited states for **T1** obtained from experiment and quantum chemical calculations (Table 1) we note that the experimental values are 0.5 eV lower; the energy difference between $^1B^*$ and $^1A^*$ excited states is predicted accurately.

For **T2** and **T3** an additional absorption band is observed in the UV at 3.7 and 3.2 eV, respectively. These absorption energies match approximately the excitation energy of the isolated oligothiophene segment. This correspondence suggests that the associated excited states, labeled S_n in Figure 6, are mainly localized on the oligothiophene segment.

For molecules **T2** and **T3** with extended π-conjugated systems, the emission spectra measured at room temperature are sensitive to solvent polarity and the emission maxima of **T2** and **T3** are slightly red shifted going from toluene to benzonitrile (0.04 eV for **T2** and 0.12 eV for **T3**) (Figure 4). In contrast, for molecule **T1**, the emission maximum (1.80 eV) does not vary with solvent polarity (Table 2). The red shift of the fluorescence maxima for molecules **T2** and **T3** with increasing solvent polarity suggests that the emitting state has charge transfer character. The solvatochromic shift for the corresponding transition in absorption ($2^1A^* \leftarrow 1^1A$) is difficult to evaluate experimentally because of the small dipole strength and the spectral overlap with the allowed ($^1B^* \leftarrow 1^1A$) transition. Intramolecular excited state charge transfer is well known for organic compounds containing carbonyl groups, e.g., coumarin dyes[74] and carotenoids.[73,75]

Electrochemical characterization in *o*-DCB shows a reduction of oligomers **T1** and **T2** near −1.11 and −1.05 V vs Ag/AgCl, respectively. Oxidation of the **T2** molecule occurs at +0.75 V vs Ag/AgCl, resulting an in electrochemical band gap of 1.8 eV for the **T2** molecule. For **T1**, no oxidation peak could be detected in the electrochemically accessible voltage range. Electrochemical measurements indicate for **T2** that an intramolecular charge transfer (CT) state with an oligothiophene substituent acting as donor and the central iDPP unit as acceptor may be expected with an energy around 2.0 eV after dielectric relaxation of the solvent around the photoexcited molecule. The presence of a CT state close in energy to the lowest excited state may account for the reduction in the rate for radiative decay from the 2^1A^* level, see Table 2. In solvents of high polarity, the CT character of the relaxed lowest excited state would increase at the expense of the vibronically admixed ^1B character. Since the transition probability mainly derives from the admixture of the $^1B^*$ state, the radiative rate is expected to go down. The increase in the rate of nonradiative decay from the lowest excited state with increasing solvent polarity may also be accounted for by the admixture of CT character. It is well known that in electron-donor acceptor dyads intersystem crossing to the triplet state can be enhanced by the energetic proximity of CT states,[76] providing a channel for nonradiative decay.

CONCLUSIONS

A series of 1,4-diaryl-3,6-di(oligothiophen-2-yl)pyrrolo[3,2-*b*]pyrrole-2,5(1*H*,4*H*)-dione (iDPP*n*T) (**T1**−**T3**) derivatives substituted with a different number of thiophene rings was synthesized. Photophysical properties were investigated using different solvents and temperatures. In contrast to the more common 3,6-di(oligothiophen-2-yl)pyrrolo[3,4-*c*]pyrrole-1,4-(2*H*,5*H*)-dione (DPP*n*T) molecules that show bright fluorescence in solution, the new isomeric iDPP*n*Ts exhibit only very weak fluorescence. For solutions of **T1**−**T3** we find that the lowest excited state of iDPP*n*T has symmetry properties (^1A) different from that of DPP*n*T (^1B) and that the transition between the ground state and the lowest excited singlet state in iDPP molecules has negligible oscillator strength. This finding is corroborated by quantum chemical calculations. Upon extending the oligothiophene moiety in the iDPP molecules, the charge transfer character of the lowest excited state becomes more pronounced. This tends to preclude high fluorescence quantum yields even in extended oligothiophene−iDPP systems.

ASSOCIATED CONTENT

Supporting Information

Synthesis, experimental procedures, and fluorescence decay curves for **T1**, **T2**, and **T3** in solvents of different polarity, and complete refs 40, 46, and 54. This material is available free of charge via the Internet at http://pubs.acs.org.

dx.doi.org/10.1021/jp400256s | *J. Phys. Chem. A* XXXX, XXX, XXX−XXX

AUTHOR INFORMATION

Corresponding Author

*E-mail: s.c.j.meskers@tue.nl.

Notes

The authors declare no competing financial interest.

ACKNOWLEDGMENTS

This research was supported by The Netherlands Organization for Scientific Research (NWO) through a grant in the VIDI scheme. S.K. is grateful to the European Marie Curie (COFUND) programme along with the Belgian science policy office ("Belspo") for current funding. D.B. and J.C. are both FNRS Research Directors.

REFERENCES

(1) Parnum, D. G.; Mehta, G.; Moore, G. G. I.; Siegal, F. P. Attempted Reformatsky Reaction of Benzonitrile, 1,4-Diketo-3,6-Diphenylpyrrolo[3,4-*c*]pyrrole. A. Lactam Analogue of Pentalene. *Tetrahedron Lett.* **1974**, *29*, 2549−2552.

(2) Nielsen, C. B.; Turbiez, M.; McCulloch, I. Recent Advances in the Development of Semiconducting DPP-Containing Polymers for Transistor Applications. *Adv. Mater.* **2012**, DOI: 10.1002/adma.201201795.

(3) Adil, D.; Kanimozhi, C.; Ukah, N.; Paudel, K.; Patil, S.; Guha, S. Electrical and Optical Properties of Diketopyrrolopyrrole-Based Copolymer Interfaces in Thin Film Devices. *ACS Appl. Mater. Interfaces* **2011**, *3*, 1463−1471.

(4) Kuwabara, J.; Yamagata, T.; Kanbara, T. Solid-State Structure and Optical Properties of Highly Fluorescent Diketopyrrolopyrrole Derivatives Synthesized by Cross-Coupling Reaction. *Tetrahedron* **2010**, *66*, 3736−3741.

(5) Rao, Y. S. Recent Advances in the Chemistry of Unsaturated Lactones. *Chem. Rev.* **1975**, *76*, 625−694.

(6) Knight, D. W. Synthetic Approaches to Butenolides. *Contemp. Org. Synth.* **1994**, *1*, 287−315.

(7) Herbst, W.; Hunger, K. *Industrial Organic Pigments*; Wiley-VCH: Weinheim, 2004.

(8) Furstenwerth, H. DE3525109A1, 1987.

(9) Langer, P.; Wuckelt, W.; Döring, M. New and Efficient Synthesis of Pyrrolo[3,2-*b*]pyrrole-2,5-Diones by Double-Anion-Capture Reactions of Ester Carbanions with Bis(imidoyl)chlorides of Oxalic Acid. *J. Org. Chem.* **2000**, *65*, 729−734.

(10) Janietz, S.; Barche, J.; Wedel, A.; Sainova, D. Poly(4-hexyl-1,2,4-triazole-4*H*): An Electron Semiconducting Analogue to Regioregular Poly(hexylthiophene). *Macromol. Chem. Phys.* **2004**, *205*, 1916−1922.

(11) Langer, P.; Döring, M. Efficient Synthesis of Nitrogen Heterocycles by Cyclization of Bis(nucleophiles) with Oxaldiimidoyl Dichlorides. *Eur. J. Org. Chem.* **2002**, *2002*, 221−234.

(12) Helmholz, F.; Schroeder, R.; Langer, P. Synthesis of Unsymmetrical Pyrrolo[3,2-*b*]pyrrole-2,5-Diones and Bis(quinazolin-4-on-2-yls) by Double-Anion-Capture Reactions of Unsymmetrical Oxaldi(arylimidoyl) Dichlorides. *Synthesis* **2006**, 2507−2514.

(13) Langer, P.; Helmholz, F.; Schroeder, R. Synthesis of Unsymmetrical Pyrrolo[3,2-*b*]pyrrole-2,5-Diones. *Synlett* **2003**, 2389−2391.

(14) Grzybowski, M.; Glodkowska-Mrowka, E.; Stoklosa, T.; Gryko, D. T. Bright, Color-Tunable Fluorescent Dyes Based on π-Expanded Diketopyrrolopyrroles. *Org. Lett.* **2012**, *14*, 2670−2673.

(15) Qu, Y.; Hua, J.; Tian, H. Colorimetric and Ratiometric Red Fluorescent Chemosensor for Fluoride Ion Based on Diketopyrrolopyrrole. *Org. Lett.* **2010**, *12*, 3320−3223.

(16) Cui, W.; Yuen, J.; Wudl, F. Benzodipyrrolidones and Their Polymers. *Macromolecules* **2011**, *44*, 7869−7873.

(17) Zhang, K. New Conjugated Polymers Based on Benzodifuranone and Diketopyrrolopyrrole. *Ph.D. Dissertation*; Verlag: Hamburg, 2012; ISBN 978-3-95425-012-7.

(18) Welterlich, I.; Charov, O.; Tieke, B. Deeply Colored Polymers Containing 1,3,4,6-Tetraarylpyrrolo[3,2-*b*]pyrrolo-2,5-Dione (IsoDPP) Units in the Main Chain. *Macromolecules* **2012**, *45*, 4511−4519.

(19) Luňák, S.; Vyňuchal, J.; Hrdina, R. Geometry and Absorption of Diketo-Pyrrolo-Pyrrole Isomers and Their π-Isoelectronic Furo-Furanone Analogues. *J. Mol. Struct.* **2009**, *919*, 239−245.

(20) Luňák, S.; Vyňuchal, J.; Hrdina, R. DFT and TD DFT Study of Isomeric Linear Benzodifuranones, Benzodipyrrolinones and Their Homologues. *J. Mol. Struct.* **2009**, *935*, 82−91.

(21) Innes, K. K.; Ross, I. G.; Moomaw, W. R. Electronic States of Azabenzenes and Azanaphthalenes: A Revised and Extended Critical Review. *J. Mol. Spectrosc.* **1988**, *132*, 492−544.

(22) Sundstrom, V.; Rentzepis, P. M.; Lim, E. C. Electronic Relaxation of Acridine as Studied by Picosecond Spectroscopy. *J. Chem. Phys.* **1977**, *66*, 4287−4293.

(23) Kohler, B. E.; Spangler, C.; Westerfield, C. The 2^1Ag State in The Linear Polyene 2,4,6,8,10,12,14,16-Octadecaoctaene. *J. Chem. Phys.* **1988**, *89*, 5422−5428.

(24) Catalán, J.; Paz, J. L.; de, G. On the Photophysics of All-Trans Polyenes: Hexatriene Versus Octatetraene. *J. Chem. Phys.* **2006**, *124*, 034306/1−11.

(25) Allen, M. T.; Whitten, D. G. The Photophysics and Photochemistry of α,ω-Diphenylpolyene Singlet States. *Chem. Rev.* **1989**, *89*, 1691−1702.

(26) Kobayashi, T.; Yasuda, M.; Okada, S.; Matsuda, H. Femtosecond Spectroscopy of a Polydiacetylene with Extended Conjugation to Acetylenic Side Groups. *Chem. Phys. Lett.* **1997**, *2267*, 472−480.

(27) Lawrence, B.; Torruellas, W.; Cha, M.; Sundheimer, M.; Stegeman, G.; Meth, J.; Etemad, S.; Baker, G. Identification and Role of Two-Photon Excited States in a π-Conjugated Polymer. *Phys. Rev. Lett.* **1994**, *73*, 597−600.

(28) Halle, S.; Yoshizawa, M.; Murata, H.; Tsutsui, T.; Saito, S.; Kobayashi, T. Ultrafast Non-Linear Optical Properties and Photo-induced Relaxation Dynamics of Poly(2,5-thienylenevinylene). *Synth. Met.* **1992**, *49*−*50*, 429−438.

(29) Birge, R. R.; Bennett, J. A.; Hubbard, L. M.; Fang, H. L.; Pierce, B. M.; Kliger, D. S.; Leroi, G. E. Two-Photon Spectroscopy of All-Trans-Retinal. Nature of the Low-Lying Singlet States. *J. Am. Chem. Soc.* **1982**, *104*, 2519−2525.

(30) Cogdell, R. J.; Frank, H. A. How Carotenoids Function in Photosynthetic Bacteria. *Biochim. Biophys. Acta* **1987**, *895*, 63−79.

(31) Mazaleyrat, J.-P.; Wakselman, M. The Williamson Reaction: A New and Efficient Method for the Alternate Resolution of 2,2′-Bis(bromomethyl)-1,1′-Binaphthyl and 1,1′-Binaphthalene-2,2′-Diol. *J. Org. Chem.* **1996**, *61*, 2695−2698.

(32) Tkachov, R.; Senkovskyy, V.; Komber, H.; Kiriy, A. Influence of Alkyl Substitution Pattern on Reactivity of Thiophene-Based Monomers in Kumada Catalyst-Transfer Polycondensation. *Macromolecules* **2011**, *44*, 2006−2015.

(33) Ono, R. J.; Kang, S.; Bielawski, C. W. Controlled Chain-Growth Kumada Catalyst Transfer Polycondensation of a Conjugated Alternating Copolymer. *Macromolecules* **2012**, *45*, 2321−2326.

(34) Ponomarenko, S. A.; Kirchmeyer, S.; Elschner, A.; Alpatova, N. M.; Halik, M.; Klauk, H.; Zschieschang, U.; Schmid, G. Decyl-End-Capped Thiophene-Phenylene Oligomers as Organic Semiconducting Materials with Improved Oxidation Stability. *Chem. Mater.* **2006**, *18*, 579−586.

(35) Carsten, B.; He, F.; Son, H. J.; Xu, T.; Yu, L. Stille Polycondensation for Synthesis of Functional Materials. *Chem. Rev.* **2011**, *111*, 1493−1528.

(36) Mazzio, K. A.; Yuan, M.; Okamoto, K.; Luscombe, C. K. Oligoselenophene Derivatives Functionalized with a Diketopyrrolopyrrole Core for Molecular Bulk Heterojunction Solar Cells. *ACS Appl. Mater. Interfaces* **2011**, *3*, 271−278.

(37) Loser, S.; Bruns, C. J.; Miyauchi, H.; Ortiz, R. P.; Facchetti, A.; Stupp, S. I.; Marks, T. J. A Naphthodithiophene-Diketopyrrolopyrrole Donor Molecule for Efficient Solution-Processed Solar Cells. *J. Am. Chem. Soc.* **2011**, *133*, 8142−8145.

(38) Lin, L.; Lu, C.; Huang, W.; Chen, Y.; Lin, H. New A-A-D-A-A-Type Electron Donors for Small Molecule Organic Solar Cells. *Org. Lett.* **2011**, *13*, 4962−4965.
(39) Osaka, I.; Shimawaki, M.; Mori, H.; Doi, I.; Miyazaki, E.; Koganezawa, T.; Takimiya, K. Synthesis, Characterization, and Transistor and Solar Cell Applications of a Naphthobisthiadiazole-Based Semiconducting Polymer. *J. Am. Chem. Soc.* **2012**, *134*, 3498−3507.
(40) Bronstein, H.; Chen, Z.; Ashraf, R. S.; Zhang, W.; Du, J.; Durrant, J. R.; Tuladhar, P. S.; Song, K.; Watkins, S. E.; Geerts, Y.; Wienk, M. M.; et al. Thieno[3,2-*b*]thiophene-Diketopyrrolopyrrole-Containing Polymers for High-Performance Organic Field-Effect Transistors and Organic Photovoltaic Devices. *J. Am. Chem. Soc.* **2011**, *133*, 3272−3275.
(41) Li, Z.; Zhang, Y.; Tsang, S.-W.; Du, X.; Zhou, J.; Tao, Y.; Ding, J. Alkyl Side Chain Impact on the Charge Transport and Photovoltaic Properties of Benzodithiophene and Diketopyrrolopyrrole-Based Copolymers. *J. Phys. Chem. C* **2011**, *115*, 18002−18009.
(42) Dou, L.; Gao, J.; Richard, E.; You, J.; Chen, C.-C.; Cha, K. C.; He, Y.; Li, G.; Yang, Y. Systematic Investigation of Benzodithiophene- and Diketopyrrolopyrrole-Based Low-Bandgap Polymers Designed for Single Junction and Tandem Polymer Solar Cells. *J. Am. Chem. Soc.* **2012**, *134*, 10071−10079.
(43) Ha, J. S.; Kim, K. H.; Choi, D. H. 2,5-Bis(2-Octyldodecyl)-Pyrrolo[3,4-*c*]pyrrole-1,4-(2*H*,5*H*)-Dione-Based Donor−Acceptor Alternating Copolymer Bearing 5,5′-Di(thiophen-2-yl)-2,2′-Biselenophene Exhibiting 1.5 $cm^2 \cdot V^{-1} \cdot s^{-1}$ Hole Mobility in Thin-Film Transistors. *J. Am. Chem. Soc.* **2011**, *133*, 10364−10367.
(44) Wu, P.-T.; Kim, F. S.; Jenekhe, S. A. New Poly(arylene vinylene)s Based on Diketopyrrolopyrrole for Ambipolar Transistors. *Chem. Mater.* **2011**, *23*, 4618−4624.
(45) Drees, M.; Facchetti, A.; Lu, S.;Yan, H. Yao, Y. Pyrrolo[3,2-*b*]pyrrole Semiconducting Compounds and Devices Incorporating Same. U.S. Patent 2011/0226338 A1, 2011.
(46) Frisch, M. J.; Trucks, G. W.; Schlegel, H. B.; Scuseria, G. E.; Robb, M. A.; Cheeseman, J. R.; Scalmani, G.; Barone, V.; Mennucci, B.; Petersson, G. A.; et al. *Gaussian 09*, Revision A.1; Gaussian Inc.: Wallingford, CT, 2009.
(47) Christiansen, O.; Koch, H.; Jørgensen, P. Response Functions in the CC3 Iterative Triple Excitation Model. *J. Chem. Phys.* **1995**, *103*, 7429−7441.
(48) Haettig, C.; Weigend, F. CC2 Excitation Energy Calculations on Large Molecules Using the Resolution of the Identity Approximation. *J. Chem. Phys.* **2000**, *113*, 5154−5161.
(49) Haettig, C.; Hald, K. Implementation of RI-CC2 Triplet Excitation Energies with an Application to Trans-Azobenzene. *Phys. Chem. Chem. Phys.* **2002**, *4*, 2111−2118.
(50) Korona, T.; Werner, H.-J. Local Treatment of Electron Excitations in the EOM-CCSD Method. *J. Chem. Phys.* **2003**, *118*, 3006−3019.
(51) Chai, J.-D.; Head-Gordon, M. Systematic Optimization of Long-Range Corrected Hybrid Density Functionals. *J. Chem. Phys.* **2008**, *128*, 084106/1−15.
(52) Henderson, T. M.; Janesko, B. G.; Scuseria, G. E. Generalized Gradient Approximation Model Exchange Holes for Range-Separated Hybrids. *J. Chem. Phys.* **2008**, *128*, 194105/1−9.
(53) Ahlrichs, R. *TURBOMOLE*, Version 5.10; University of Karlsruhe, 2008.
(54) Werner, H.-J.; Knowles, P. J.; Manby, F. R.; Schütz, M.; Celani, P.; Knizia, G.; Korona, T.; Lindh, R.; Mitrushenkov, A.; Rauhut, G.; et al. *Molpro, version 2009.1, a package of ab initio programs*; University College Cardiff Consultants Limited: Wales, U.K., 2010; http://www.molpro.net.
(55) Shao, Y.; et al. Advances in Methods and Algorithms in a Modern Quantum Chemistry Program Package. *Phys. Chem. Chem. Phys.* **2006**, *8*, 3172−3191.
(56) Peach, M. J.; Benfield, P.; Helgaker, T.; Tozer, D. J. Excitation Energies in Density Functional Theory: An Evaluation and a Diagnostic Test. *J. Chem. Phys.* **2008**, *128*, 044118.
(57) Strickler, S. J.; Berg, R. A. Relationship Between Absorption Intensity and Fluorescence Lifetime of Molecules. *J. Chem. Phys.* **1962**, *37*, 814−822.
(58) Kirkus, M.; Wang, L.; Mothy, S.; Beljonne, D.; Cornil, J.; Janssen, R. A. J.; Meskers, S. C. J. Optical Properties of Oligothiophene Substituted Diketopyrrolopyrrole Derivatives in the Solid Phase: Joint J- and H-Type Aggregation. *J. Phys. Chem. A* **2012**, *116*, 7927−7936.
(59) Janssen, R. A. J.; Smilowitz, L.; Sariciftci, N. S.; Moses, D. Triplet-State Photoexcitations of Oligothiophene Films and Solutions. *J. Chem. Phys.* **1994**, *101*, 1787−1798.
(60) van Gompel, J. A.; Schuster, G. B. Photophysical Behavior of Ester-Substituted Aminocoumarins: a New Twist. *J. Phys. Chem.* **1989**, *93*, 1292−1295.
(61) Varadarajan, T. S. Substituent and Solvent Effects on the Twisted Intramolecular Charge Transfer of Three New 7-(Diethylamino)coumarin-3-Aldehyde Derivatives. *J. Phys. Chem.* **1994**, *98*, 8903−8905.
(62) López Arbeloa, T.; López Arbeloa, F.; Tapia Estévez, M. J.; López Arbeloa, I. Binary Solvent Effects on the Absorption and Emission of 7-Aminocoumarins. *J. Lumin.* **1994**, *59*, 369−375.
(63) Nag, A.; Kundu, T.; Bhattacharyya, K. Effect of Solvent Polarity on the Yield of Twisted Intramolecular Charge Transfer (TICT) Emission. Competition Between Formation and Nonradiative Decay of the TICT State. *Chem. Phys. Lett.* **1989**, *160*, 257−260.
(64) Raju, B. B. Photophysical Properties of Ground-State Twisted Bicoumarins. *J. Phys. Chem. A* **1997**, *5639*, 981−987.
(65) Rurack, K.; Spieles, M. Fluorescence Quantum Yields of a Series of Red and Near-Infrared Dyes Emitting at 600−1000 nm. *Anal. Chem.* **2011**, *83*, 1232−1242.
(66) Das, P. K.; Becker, R. S. Spectroscopy of Polyenes. 6. Absorption and Emission Spectral Properties of Linear Polyenals of the Series CH_3-$(CH{:}CH)_n$-CHO. *J. Phys. Chem.* **1982**, *86*, 921−927.
(67) Ros, M.; Groenen, E. J. J.; Hemert, M. C. V. Ab Initio Calculations on the Lower Excited States of Short-Chain Polyenals. *J. Am. Chem. Soc.* **1992**, *6*, 6820−6827.
(68) Yamaguchi, S.; Tahara, T. Two-Photon Absorption Spectrum of All-Trans Retinal. *Chem. Phys. Lett.* **2003**, *376*, 237−243.
(69) Takeuchi, S.; Tahara, T. Ultrafast Fluorescence Study on the Excited Singlet-State Dynamics of All-Trans-Retinal. *J. Phys. Chem. A* **1997**, *101*, 3052−3060.
(70) Vivas, M. G.; Silva, D. L.; Misoguti, L.; Zaleśny, R.; Bartkowiak, W.; Mendonca, C. R. Degenerate Two-Photon Absorption in All-Trans Retinal: Nonlinear Spectrum and Theoretical Calculations. *J. Phys. Chem. A* **2010**, *114*, 3466−3470.
(71) Hudson, B. S.; Loda, R. T. Spectroscopy of 2,4,6,8,10-Dodecapentaenal: Laser Site Selection of a Retinal Analog. *Chem. Phys. Lett.* **1981**, *81*, 591−594.
(72) Frank, H. A.; Bautista, J. A.; Josue, J.; Pendon, Z.; Hiller, R. G.; Sharples, F. P.; Gosztola, D.; Wasielewski, M. R. Effect of the Solvent Environment on the Spectroscopic Properties and Dynamics of the Lowest Excited States of Carotenoids. *J. Phys. Chem. B* **2000**, *104*, 4569−4577.
(73) Zigmantas, D.; Hiller, R. G.; Sharples, F. P.; Frank, H. A.; Sundstrom, V.; Polivka, T. Effect of a Conjugated Carbonyl Group on the Photophysical Properties of Carotenoids. *Phys. Chem. Chem. Phys.* **2004**, *6*, 3009−3016.
(74) Jones, G., II; Jackson, W. R.; Choi, C.; Bergmark, W. R. Solvent Effects on Emission Yield and Lifetime for Coumarin Laser Dyes. Requirements for a Rotatory Decay Mechanism. *J. Phys. Chem.* **1985**, *89*, 294−300.
(75) Polívka, T.; Sundström, V. Ultrafast Dynamics of Carotenoid Excited States−From Solution to Natural and Artificial Systems. *Chem. Rev.* **2004**, *104*, 2021−2072.
(76) Dance, Z. E. X.; Mi, Q.; McCamant, D. W.; Ahrens, M. J.; Ratner, M. A.; Wasielewski, M. R. Time-Resolved EPR Studies of Photogenerated Radical Ion Pairs Separated by p-Phenylene Oligomers and of Triplet States Resulting From Charge Recombination. *J. Phys. Chem. B* **2006**, *110*, 25163−25173.